

# Balanced MSM-2DEG Varactors Based on AlGaN/GaN Heterostructure With Cutoff Frequency of 1.54 THz

Ji Hyun Hwang, Kye-Jeong Lee, Sung-Min Hong, *Member, IEEE*, and Jae-Hyung Jang, *Member, IEEE*

**Abstract**—AlGaN/GaN high-electron mobility transistor structures were utilized to fabricate metal–semiconductor–metal (MSM) two-dimensional electron gas (2DEG) varactors for application as a terahertz (THz) capacitive switch. By adopting an asymmetric MSM structure composed of nanoscale gates and micron-scale gates, the cutoff frequency of the MSM-2DEG varactors was dramatically improved, up to the THz range, by reducing series resistance. The balanced MSM-2DEG varactor, in which a nanoscale gate is sandwiched between two micron-scale gates exhibited a capacitance switching ratio ( $C_{\max}/C_{\min}$ ) of 2.64, a cutoff frequency of 1.54 THz, and a figure of merit of 4.06 THz.

**Index Terms**—Terahertz, gallium nitride, high electron mobility transistor (HEMT), asymmetric, balanced, and metal–semiconductor–metal (MSM)-2DEG varactors.

## I. INTRODUCTION

SOLID-STATE electronic devices in the past decade have made great progress in high frequency applications, reaching up to the terahertz (THz) frequency range [1]–[3]. Since THz electronic circuits such as voltage controlled oscillators [4], [5] and multipliers [6], [7] need varactor diodes, studies on varactors have been carried out to improve their highly nonlinear capacitance-voltage (C-V) characteristics [8] and to push their cutoff frequency up into the THz frequency range [9]. Recently, varactor diodes have been utilized as control elements in THz modulators, based on active metamaterials composed of split ring resonators, whose capacitances are switched by the integrated MSM varactors [10]. For capacitance switching elements in the THz frequency range, vertical or lateral Schottky diodes [11], [12] and heterostructure barrier varactors [13], [14] have typically been used. On the other hand, planar metal–semiconductor–metal (MSM) two-dimensional electron gas (2DEG) varactors have simpler structures, and advantages such as steep capacitance switching, bi-stable operation, low leakage current, and HEMT compatible process. However, the MSM-2DEG varactors suffer from relatively low cutoff frequency due to their large associated series resistance.

Many studies on MSM-2DEG varactors have investigated ways of increasing their cutoff frequency for possi-

Manuscript received November 8, 2016; accepted November 13, 2016. Date of publication November 16, 2016; date of current version December 27, 2016. This work was supported by the Samsung Research Funding Center of Samsung Electronics under Project SRFC-IT1401-08. The review of this letter was arranged by Editor A. V. Y. Thean.

The authors are with the School of Electrical Engineering and Computer Science, Gwangju Institute of Science and Technology, Gwangju 500-712, South Korea (e-mail: jjang@gist.ac.kr).

Color versions of one or more of the figures in this letter are available online at <http://ieeexplore.ieee.org>.

Digital Object Identifier 10.1109/LED.2016.2628866

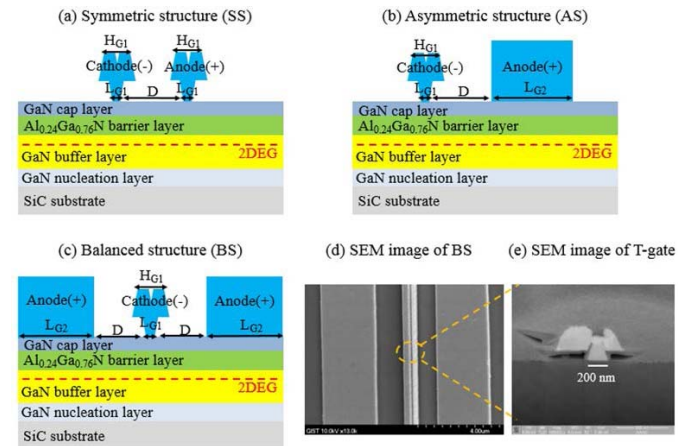


**Fig. 1.** Cross-sectional schematic of MSM-2DEG varactors with (a) symmetric structure (SS) with two nanoscale T-gates; (b) asymmetric structure (AS); and (c) balanced structure (BS). (d) Top-view SEM image of the BS-type varactor (e) Cross-sectional SEM image of a 200-nm-long T-gate. All dimensions were designed as follows;  $L_{G1} = 200$  nm,  $H_{G1} = 500$  nm,  $L_{G2} = 3 \mu\text{m}$ , and  $D = 1 \mu\text{m}$ .

ble THz application. In one approach, two Schottky gates and their gate spacing were scaled down to achieve small capacitance and resistance. AlGaN/GaN-based MSM-2DEG varactors with a cutoff frequency of 74 GHz [15], InP/InGaAs-based MSM-2DEG varactors with a cutoff frequency of 0.9 THz [16], and InAlN/GaN-based MSM-2DEG varactors with a cutoff frequency of 0.3 THz [17] have been reported, using 500-nm-long rectangular gates, 130-nm-long T-gates, and 90-nm-long T-gates, respectively. However, the lateral scaling approach will no longer be effective because of the reduction in capacitance switching ratio, in combination with the increased resistance. As the gate length is scaled down to less than 100 nm, metal–semiconductor interfacial resistance becomes dominant in the total resistance and offsets the reduced gate capacitance. Therefore, the resultant cutoff frequency cannot be further improved with the shorter gate length. Furthermore,  $C_{\max}/C_{\min}$  will also deteriorate as the gate length decreases.

In this work, MSM-2DEG varactors with symmetric, asymmetric, and balanced structures have been fabricated, as shown in Figs. 1(a) to 1(c). Conventional MSM-2DEG varactors, which have a symmetric structure (SS) based on two nanoscale T-gates, have had difficulties achieving sub-micron gate spacing and low resistance. By employing an asymmetric structure (AS) and a balanced structure (BS) that adopt alternating micron-scale rectangular gates and nanoscale T-gates, the associated series resistance was dramatically reduced, while retaining low capacitance and bi-stable operating char-

acteristics. Both the AS- and BS-type MSM-2DEG varactors take advantage of the low resistance of micron-scale gates, and the low capacitance of nanoscale gates. The fabricated AlGaN/GaN-based BS-type MSM-2DEG varactors demonstrated a cutoff frequency of 1.54 THz,  $C_{\max}/C_{\min}$  of 2.64, and a figure of merit (FOM) of 4.06 THz.

## II. FABRICATION OF THE MSM-2DEG VARACTORS

An epitaxial structure was grown on a SiC substrate consisting of an AlN nucleation layer, a 1.8- $\mu\text{m}$  Fe-doped GaN buffer layer, a 22-nm-thick  $\text{Al}_{0.24}\text{Ga}_{0.76}\text{N}$  Schottky barrier layer, and a 3-nm-thick GaN cap layer, from the bottom to the top. The heterostructures were grown by metal-organic chemical vapor deposition (MOCVD). The Hall measurements yielded a 2DEG sheet charge density of  $9.51 \times 10^{12} \text{ cm}^{-2}$  and an electron mobility of  $1,430 \text{ cm}^2/\text{V}\cdot\text{s}$  at room temperature.

The fabrication began with mesa-isolation using inductively-coupled-plasma reactive-ion-etching (ICP-RIE) with  $\text{Cl}_2$ -based chemistry. Microwave probe pads were deposited with Ti/Au (20/300 nm) metallization. The 3- $\mu\text{m}$ -long rectangular gates were fabricated by optical lithography and Ni/Au (20/300 nm) metallization. A tri-layer of e-beam resist stack consisting of ZEP520A/PMGI-SF8 /ZEP520A was utilized with subsequent e-beam lithography to delineate the 200-nm-long T-gates. After double exposures and develops, a Ni/Au (20/350 nm) gate was evaporated and lifted-off. All the gates had a common width ( $W$ ) of 20  $\mu\text{m}$ .

The top-view scanning electron microscopy (SEM) image of the BS-type MSM-2DEG varactor and a cross-sectional SEM image of the 200-nm-long T-gate are shown in Fig. 1(d) and 1(e), respectively. Compared to the SS sample, which has two 200-nm-long T-gates, the AS design has a 200-nm-long T-gate and a 3- $\mu\text{m}$ -long rectangular gate. The 3- $\mu\text{m}$ -long gate reduces the metal-semiconductor interfacial resistance [18] which dominates the series resistance in the MSM-2DEG varactors. The BS-type MSM-2DEG varactors had a 200-nm-long T-gate between two 3- $\mu\text{m}$ -long rectangular gates, which reduced the 2DEG channel resistance, another component of the series resistance in MSM-2DEG varactors [17].

## III. RESULTS AND DISCUSSION

The DC current-voltage characteristics of the MSM-2DEG varactors were measured with an Agilent 4155A and are shown in Fig. 2. The 3- $\mu\text{m}$ -long gate shows an order of magnitude higher gate leakage current ( $\sim 1 \times 10^{-8} \text{ A/mm}$ ) than that of the 200-nm-long T-gate ( $\sim 1 \times 10^{-9} \text{ A/mm}$ ) in the negative voltage region. The gate leakage current in the negative voltage region is proportional to the size of the anodes, which are reverse biased. The SS-, AS-, and BS-type MSM-2DEG varactors exhibit essentially the same gate leakage current in the positive voltage region, where cathodes with the same gate length are reverse biased. To investigate the capacitance-voltage (C-V) characteristics of the AlGaN/GaN-based MSM-2DEG varactors, S-parameters were measured from 1 GHz to 40 GHz with a HP8510C vector network analyzer. The effects of the probe pads were de-embedded by using on-wafer open patterns. An equivalent circuit of the MSM-2DEG varactors composed of a series resistance ( $R$ ), an inductance ( $L$ ), a capacitance ( $C$ ), and a parallel conductance ( $G$ ) was used to fit the measurement results [15]. The modeled S-parameters agreed very well with the measured S-parameters for the BS-type

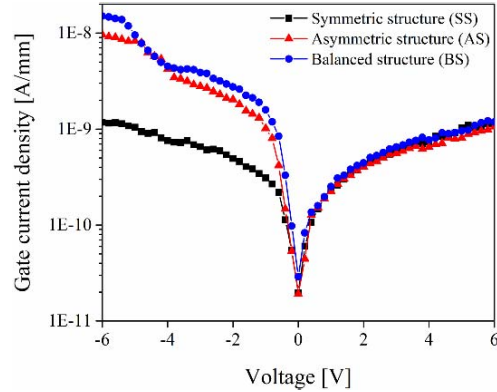


Fig. 2. DC current-voltage characteristics of the SS-, AS-, and BS-type MSM-2DEG varactors.

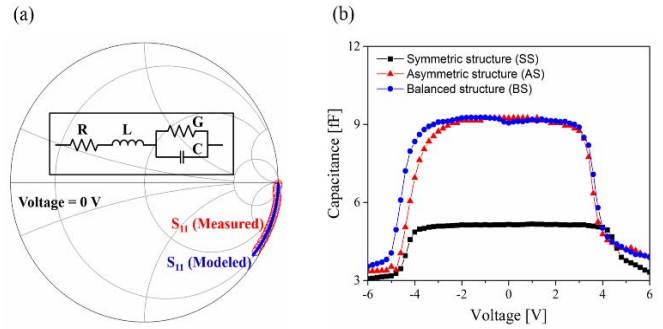


Fig. 3. (a) Measured (open red circles) and modeled (blue solid line)  $S_{11}$  of the BS-type MSM-2DEG varactors. The inset shows the equivalent circuit of the MSM-2DEG varactors. (b) Capacitance-voltage (C-V) characteristics of the MSM-2DEG varactors.

MSM-2DEG varactors, as shown in Fig. 3(a). The C-V characteristics of the MSM-2DEG varactors are shown in Fig. 3(b). The AS- and BS-type devices exhibit a larger capacitance than the SS-type devices at the zero bias voltage, where the two Schottky capacitances associated with the anode and cathode electrodes are series-connected. For the SS-type devices, the maximum capacitance at the zero bias voltage is determined by the series-connected two Schottky capacitance associated with 200-nm-long T-gates. On the other hand, the AS- and BS-type devices exhibit essentially the same maximum capacitance value, which is determined by the single 200-nm-long T-gate, whose Schottky capacitance is much smaller than that of the 3- $\mu\text{m}$ -long gate. Various electrical parameters of the MSM-2DEG varactors are summarized in Table I, where the parameters were extracted from more than 20 devices for each type of MSM-2DEG varactors.

The cutoff frequency of the MSM-2DEG varactors is defined as  $f_0 = 1/(2\pi R_0 C_0)$ , where  $R_0$  and  $C_0$  are resistance and capacitance under the zero bias voltage [13]–[15]. The figure of merit (FOM) is defined as  $f_0 \cdot (C_{\max}/C_{\min})$ .

Considering that the SS-type MSM-2DEG varactors with 200-nm-long rectangular gates, and the varactors with 200-nm-long T-gates, have maximum capacitances of 3.51 fF and 5.03 fF, respectively, the fringing capacitance associated with the head of the T-gates for the SS-type is estimated to be 1.52 fF, which matches well with the simulation results shown in [12]. When the fringing capacitance is excluded, it is noticed that the AS- and BS-type MSM-2DEG varactors have almost two times larger capacitance value than the SS-type MSM-2DEG varactors at the zero bias voltage. Employing the

TABLE I

SUMMARY OF VARIOUS ELECTRICAL PROPERTIES OF FABRICATED MSM-2DEG VARACTORS WITH DIFFERENT STRUCTURES; NS, AS, AND BS

	$C_{\max}$ [fF]	$C_{\min}$ [fF]	$R_0$ ( $\Omega$ )	C-ratio ( $C_{\max}/C_{\min}$ )	$f_0$ [THz]	FOM [THz]	$C_{\max}/W$ [fF/ $\mu\text{m}$ ]
SS	5.03 ( $\pm 0.20$ )	3.07 ( $\pm 0.12$ )	27.3 ( $\pm 0.37$ )	1.64 ( $\pm 0.05$ )	1.16 ( $\pm 0.05$ )	1.90 ( $\pm 0.07$ )	0.25 ( $\pm 0.01$ )
AS	9.04 ( $\pm 0.13$ )	3.28 ( $\pm 0.11$ )	16.7 ( $\pm 0.34$ )	2.75 ( $\pm 0.12$ )	1.05 ( $\pm 0.03$ )	2.90 ( $\pm 0.13$ )	0.45 ( $\pm 0.01$ )
BS	9.08 ( $\pm 0.12$ )	3.44 ( $\pm 0.10$ )	11.4 ( $\pm 0.52$ )	2.64 ( $\pm 0.09$ )	1.54 ( $\pm 0.08$ )	4.06 ( $\pm 0.20$ )	0.45 ( $\pm 0.01$ )

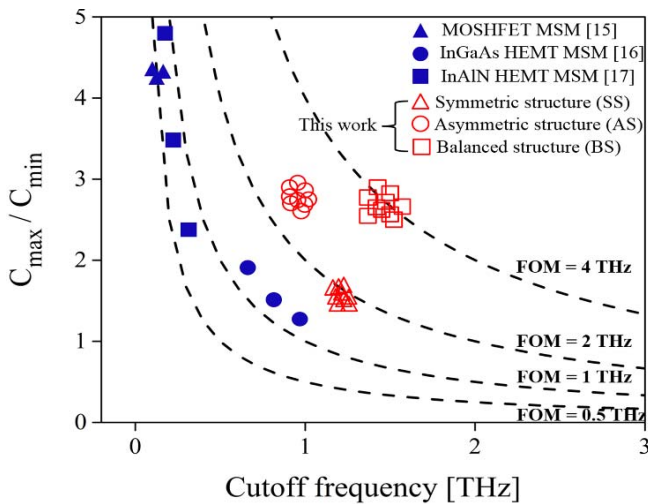


Fig. 4. Capacitance switching ratio and the cutoff frequencies of the MSM-2DEG varactors with different device structures and other reported values.

T-gates increases the associated fringing capacitance, but it significantly reduces the gate resistance at high frequency. The SS-type MSM-2DEG varactor with 200-nm-long rectangular gates exhibits a series resistance of  $67.5 \Omega$ , whereas those with the 200-nm-long T-gates exhibits a series resistance of  $27.3 \Omega$ . Accordingly, the resulting cutoff frequency of the devices with T-gates (1.16 THz) is higher than that of the devices with rectangular gates (0.67 THz).

When we compare the series resistance values of the three types of devices, it is clear that the AS- and BS-type MSM-2DEG varactors have a significantly smaller series resistance than the SS-type devices. By employing a larger gate at the anode of the AS-type MSM-2DEG varactor, the series resistance can be minimized, because the contact resistance and the metal resistance of the devices are reduced. The BS-type MSM-2DEG varactor exhibits a lower series resistance than the AS-type MSM-2DEG varactor because the resistance associated with the 2DEG channel is halved in the BS-type MSM-2DEG varactor. The resistance associated with the 2DEG channel can also be reduced by fabricating the devices with a smaller gate spacing [17].

The highest cutoff frequency and FOM was demonstrated by the BS-type MSM-2DEG varactors. They exhibited a  $f_0$  of 1.54 THz,  $C_{\max}/C_{\min}$  of 2.64, and a FOM of 4.06 THz. Fig. 4 shows the capacitance switching ratio versus the cutoff frequency. The dotted lines are the constant figure of merit (FOM) curves. It can be clearly observed that the

BS-type varactors have effectively enhanced high frequency characteristics, compared to the SS or AS-type MSM-2DEG varactors. In particular, the BS-type MSM-2DEG varactors in this work showed a record-high cutoff frequency and FOM, compared to previous studies on MSM-2DEG varactors, whose cutoff frequencies were below 1 THz [15]–[17].

#### IV. CONCLUSION

The electrical characteristics of AlGaN/GaN-based MSM-2DEG varactors with asymmetric and balanced structures were investigated. By employing a balanced gate structure comprised of a 200-nm-long T-gate between two 3- $\mu\text{m}$ -long rectangular gates, a cutoff frequency of 1.54 THz, a capacitance switching ratio of 2.64, and a FOM of 4.06 THz were achieved. The MSM-2DEG varactors can be utilized in control elements in a THz modulator operating at a frequency higher than 1 THz.

#### REFERENCES

- [1] T. Nagatsuma, G. Ducournau, and C. C. Renaud, “Advances in terahertz communications accelerated by photonics,” *Nature Photon.*, vol. 10, pp. 371–379, Jun. 2016, doi: 10.1038/nphoton.2016.65.
- [2] M. Tonouchi, “Cutting-edge terahertz technology,” *Nature Photon.*, vol. 1, pp. 97–105, Feb. 2007, doi: 10.1038/nphoton.2007.3.
- [3] B. Ferguson and X.-C. Zhang, “Materials for terahertz science and technology,” *Nature Mater.*, vol. 1, pp. 26–33, Sep. 2002, doi: 10.1038/nmat708.
- [4] S. Kitagawa, S. Suzuki, and M. Asada, “650-GHz resonant-tunneling-diode VCO with wide tuning range using varactor diode,” *IEEE Electron Device Lett.*, vol. 35, no. 12, pp. 1215–1217, Dec. 2014, doi: 10.1109/LED.2014.2364826.
- [5] M. Seo, M. Urteaga, J. Hacker, A. Young, Z. Griffith, V. Jain, R. Pierson, P. Rowell, A. Skalare, A. Peralta, R. Lin, D. Pukala, and M. Rodwell, “InP HBT IC technology for terahertz frequencies: Fundamental oscillators up to 0.57 THz,” *IEEE J. Solid-State Circuits*, vol. 46, no. 10, pp. 2203–2214, Oct. 2011, doi: 10.1109/JSSC.2011.2163213.
- [6] A. Maestrini, I. Mehdi, J. V. Siles, J. S. Ward, R. Lin, B. Thomas, C. Lee, J. Gill, G. Chattopadhyay, E. Schlecht, J. Pearson, and P. Siegel, “Design and characterization of a room temperature all-solid-state electronic source tunable from 2.48 to 2.75 THz,” *IEEE Trans. THz Sci. Technol.*, vol. 2, no. 2, pp. 177–185, Mar. 2012, doi: 10.1109/TTHZ.2012.2183740.
- [7] J. V. Siles and J. Grajal, “Physics-based design and optimization of Schottky diode frequency multipliers for terahertz applications,” *IEEE Trans. Microw. Theory Techn.*, vol. 58, no. 7, pp. 1933–1942, Jul. 2010, doi: 10.1109/TMTT.2010.2050103.
- [8] X. Zhao *et al.*, “Optically modulated high-sensitivity heterostructure varactor,” *IEEE Electron Device Lett.*, vol. 27, no. 9, pp. 710–712, Sep. 2006, doi: 10.1109/LED.2006.880637.
- [9] D. Shim and K. O. Kenneth, “Symmetric varactor in 130-nm CMOS for frequency multiplier applications,” *IEEE Electron Device Lett.*, vol. 32, no. 4, pp. 470–472, Apr. 2011, doi: 10.1109/LED.2011.2108994.
- [10] M. T. Nouman, H.-W. Kim, J. M. Woo, J. H. Hwang, D. Kim, and J.-H. Jang, “Terahertz modulator based on metamaterials integrated with metal-semiconductor-metal varactors,” *Sci. Rep.*, vol. 6, p. 26452, May 2016, doi: 10.1038/srep26452.
- [11] C. Jin, “GaN Schottky diodes for signal generation and control,” Ph.D. dissertation, IEMN, Univ. Lille, Villeneuve-d’Ascq, France, 2015.
- [12] K. Shinohara, D. C. Regan, Y. Tang, A. L. Corrion, D. F. Brown, J. C. Wong, J. F. Robinson, H. H. Fung, A. Schmitz, T. C. Oh, S. J. Kim, P. S. Chen, R. G. Nagele, A. D. Margomenos, and M. Micovic, “Scaling of GaN HEMTs and Schottky diodes for submillimeter-wave MMIC applications,” *IEEE Trans. Electron Devices*, vol. 60, no. 10, pp. 2982–2996, Oct. 2013, doi: 10.1109/TED.2013.2268160.
- [13] A. Reklaitis, “Terahertz-frequency InN/GaN heterostructure-barrier varactor diodes,” *J. Phys. Condens. Matter*, vol. 20, no. 38, p. 384202, Aug. 2008, doi: 10.1088/0953-8984/20/38/384202.
- [14] M. Saglam *et al.*, “High-performance 450-GHz GaAs-based heterostructure barrier varactor tripler,” *IEEE Electron Device Lett.*, vol. 24, no. 3, pp. 138–140, Mar. 2003, doi: 10.1109/LED.2003.809042.

- [15] M. Marso, A. Fox, G. Heidelberger, P. Kordos, and H. Luth, "Comparison of AlGaN/GaN MSM varactor diodes based on HFET and MOSHFET layer structures," *IEEE Electron Device Lett.*, vol. 27, no. 12, pp. 945–947, Dec. 2006, doi: 10.1109/LED.2006.886705.
- [16] S. H. Shin, D.-M. Geum, and J.-H. Jang, "MSM varactor diodes based on In<sub>0.7</sub>Ga<sub>0.3</sub>As HEMTs with cut-off frequency of 908 GHz," *IEEE Electron Device Lett.*, vol. 35, no. 2, pp. 172–174, Feb. 2014, doi: 10.1109/LED.2013.2292933.
- [17] D.-M. Geum, S. H. Shin, S.-M. Hong, and J.-H. Jang, "Metal-semiconductor-metal varactors based on InAlN/GaN heterostructure with cutoff frequency of 308 GHz," *IEEE Electron Device Lett.*, vol. 36, no. 4, pp. 306–308, Apr. 2015, doi: 10.1109/LED.2015.2400447.
- [18] H. Rohdin, N. Moll, C. Su, and G. S. Lee, "Interfacial gate resistance in Schottky-barrier-gate field effect transistors," *IEEE Trans. Electron Devices*, vol. 45, no. 12, pp. 2407–2416, Dec. 1998, doi: 10.1109/16.735716.